Journal of Applied Mechanics and Technical Physics, Vol. 49, No. 3, pp. 442–453, 2008

MIXING DYNAMICS OF A VAPOR-CONDENSATE CLOUD WITH THE AMBIENT AIR

I. M. Bayanov, I. R. Khamidullin, and V. Sh. Shagapov

UDC 551.511+533

The mixing of a wet vapor with a gas is studied using analytical and numerical models. The one-dimensional problem of diffusion mixing accompanied by phase transitions is solved in a self-similar formulation. The versions of mixing of the vapor with a cold and warm gas and with a superheated vapor are analyzed. The atmospheric diffusion of immediate emissions containing water vapor and condensate is modeled numerically in a three-dimensional formulation. A study is made of the evolution of hydrodynamic, concentration, and temperature fields as a function of the initial emission parameters (temperature and humidity) and ambient air parameters.

Key words: *diffusion of industrial emissions, surface layer of the atmosphere, condensate, vaporization.*

INTRODUCTION

As a rule, industrial emissions to the atmosphere are multiphase medium which has a temperature different from the ambient temperature and contains gas impurities and suspended liquid and solid microparticles [1]. Entering the atmosphere at lower temperature, various emission components can be condensed by mixing with a colder medium or combine with the atmospheric moisture to form liquid droplets, i.e., liquid aerosols [2]. A mixture of a vapor, air, and aerosol will be called a mist. Propagating further and mixing with dry air, the mist cloud is gradually rising or vaporizing. The development of this process depends on many factors [3, 4], the main of which are apparently the temperature and droplet concentration in the emission cloud and the temperature and vapor partial density in the ambient air.

The main processes determining the dynamics of the cloud occur at the interface between the mixing zone and the ambient air, where the gradients of the hydrodynamic and thermodynamic quantities have the largest values. These complex effects of heat and mass transfer and phase transitions are analyzed using simple models. The plane one-dimensional problem of diffusion mixing of gas–vapor–droplet and gas–vapor mixtures is solved. A more detailed analysis of the process with the convective and turbulent transfer of mass, momentum, and heat over the entire volume of the cloud is conducted by numerical solution of the equations of fluid dynamics.

PROBLEM OF DIFFUSION MIXING OF A MIST WITH A GAS IN A ONE-DIMENSIONAL FORMULATION

Constitutive Equations. Let a gas–vapor–droplet mixture at temperature T_{v0} and partial droplet density ρ_{l0} in the initial state (mist region) occupy the semi-infinite region on the left of a fictitious boundary

Birsk State Social-Pedagogical Academy, Birsk 452453; bim1966@mail.ru; ildar_kh_r@rambler.ru, shagapov@rambler.ru. Translated from Prikladnaya Mekhanika i Tekhnicheskaya Fizika, Vol. 49, No. 3, pp. 114–127, May–June, 2008. Original article submitted January 24, 2007; revision submitted July 15, 2007.

($-\infty < x < 0$), and let a gas–vapor mixture at temperature T_{v0} and vapor partial density ρ_{l0} (gas region) occupy the region on the right of the boundary ($0 \leqslant x < +\infty$). At the initial time ($t = 0$), the partition is removed, resulting in diffusion mixing, accompanied by condensation and droplet vaporization. In all regions, the pressure is uniform and equal to the normal atmospheric pressure: $P = P_a$. Then, the initial ($t = 0$) conditions are given by

$$\begin{aligned} &x < 0: \qquad T = T_{v0}, \quad \rho_v = \rho_{v0}, \quad \rho_g = \rho_{g0}, \quad \rho_l = \rho_{l0}, \\ &x \geqslant 0: \qquad T = T_{g0}, \quad \rho_v = \rho_{v1}, \quad \rho_g = \rho_{g1}, \quad \rho_l = 0. \end{aligned} \tag{1}$$

For a theoretical description of the mixing process, we adopt the following assumptions. The volume concentration of liquid droplets is low ($\alpha_l \ll 1$), and they do not prevent mixing in a diffusion regime according to Fick's law [5]

$$\rho_g v_g = -D \frac{\partial \rho_g}{\partial x} \tag{2}$$

(ρ_g and v_g are the partial density and diffusion velocity of the gas, respectively, and D is the diffusion coefficient). Mixing occurs in an equilibrium regime for phase transitions (in the region containing the liquid droplets, the temperature and partial pressure of the vapor satisfy the Clapeyron–Clausius equation). We assume that the liquid droplets do not participate in the diffusion ($v_l = 0$). We also assume that the total pressure remains constant during the diffusion mixing.

Under the above assumptions, the mass conservation law for the gas and Fick's law (2) lead to the diffusion equation

$$\frac{\partial \rho_g}{\partial t} = D \frac{\partial^2 \rho_g}{\partial x^2}. \tag{3}$$

In the one-temperature approximation for the mist region ($x < x_s$), the heat-input equation is written as

$$\rho c \frac{\partial T}{\partial t} = \lambda \frac{\partial^2 T}{\partial x^2} + l \frac{\partial \rho_l}{\partial t}, \qquad \rho c = \rho_g c_g + \rho_v c_v + \rho_l c_l, \tag{4}$$

where T is the temperature of the mixture; ρc is the heat capacity per unit volume of the gas–vapor–liquid system, which is determined with the component mass fraction taken into account, λ is the thermal conductivity of the system, l is the specific heat of the phase transition, c_g, c_v, and c_l are the specific heats of the gas, vapor, and liquid, respectively, ρ_v and ρ_g are the partial densities of the vapor and gas, and ρ_l is the partial density of the droplets, which is determined as the total droplet mass in the unit volume of the mixture. The last term in the first expression (4) takes into account the heat effect of phase transitions.

The pressure of the mixture is determined by the partial pressures of the gas and vapor according to Dalton law:

$$P = P_g + P_v. \tag{5}$$

The partial pressures of the vapor and gas are found from the relations

$$P_v = \rho_v RT/\mu_v, \qquad P_g = \rho_g RT/\mu_g, \tag{6}$$

where R is the universal gas constant and μ_v and μ_g are the molar weights of the vapor and gas.

In the mist region, the partial pressure of the vapor P_v is equal to the saturated-vapor pressure $P_s(T)$ at the current temperature [$P_v = P_s(T)$]. This dependence is determined from the expression [6]

$$P_s(T) = P_* \exp(-T_*/T), \tag{7}$$

where P_* and T_* are empirical parameters obtained from tabular data. According to (5) and (6), the vapor and gas densities in the mixture are uniquely expressed in terms of the current temperature:

$$\rho_v = \mu_v P_s(T)/(RT), \qquad \rho_g = \mu_g (P - P_s(T))/(RT). \tag{8}$$

The equations given above are supplemented by relations at the interface between the regions. In the cross section $x = x_s$, the condition of continuity of the partial density ρ_g and (according to the mass conservation law for the air) the equality of mass fluxes are satisfied:

$$\rho_g^- = \rho_g^+, \qquad -D\Big(\frac{\partial \rho_g}{\partial x}\Big)^- + D\Big(\frac{\partial \rho_g}{\partial x}\Big)^+ = 0. \tag{9}$$

The minus and plus superscripts correspond to the parameters on the left and right of the interface, respectively.

At the interface $x = x_s$, it is assumed that the temperature is continuous and the partial density of droplets is nonzero ($\rho_l \neq 0$). The temperature continuity condition and the heat-balance equation lead to

$$T^- = T^+ = T_s, \qquad -\lambda\Big(\frac{\partial T}{\partial x}\Big)^- + \lambda\Big(\frac{\partial T}{\partial x}\Big)^+ = -\dot{x}_s \rho_l l. \tag{10}$$

Formulation of the Problem in a Self-Similar Formulation. Problem (3), (4) with boundary conditions (9) and (10) and initial conditions (1) is self-similar [7]. This formulation is a generalization of the Stefan problem [8] because it is assumed that phase transitions can occur not only on the boundaries of the fronts but also in the volume zones.

As a rule, during transfer in gases, the Lewis number is close to unity ($\mathrm{Le} = D\rho c/\lambda \approx 1$); therefore, the diffusion coefficient and thermal diffusivity will be considered constant and equal [$D = \lambda/(\rho c)$]. Let us introduce the dimensionless self-similar variable

$$\xi = x/(2\sqrt{Dt}\,).$$

Then, Eq. (3) is written as

$$-2\xi \frac{d\rho_g}{d\xi} = \frac{d^2\rho_g}{d\xi^2}. \tag{11}$$

In the mist region, the heat-conduction equation (4) becomes

$$-2\xi \frac{dT}{d\xi} = \frac{d^2T}{d\xi^2} - 2\xi \frac{l}{\rho c} \frac{d\rho_l}{d\xi}. \tag{12}$$

Using the self-similar variable, the boundary conditions (9) and (10) at the point $\xi_s = x_s/(2\sqrt{Dt}\,)$ are written as

$$\begin{gathered} -D\Big(\frac{\partial \rho_g}{\partial x}\Big)^-_{\xi_s} + D\Big(\frac{\partial \rho_g}{\partial x}\Big)^+_{\xi_s} = 0, \\ T^- = T^+ = T_s, \qquad -\Big(\frac{dT}{d\xi}\Big)^-_{\xi_s} + \Big(\frac{dT}{d\xi}\Big)^+_{\xi_s} = -2\xi \frac{\rho_l l}{\rho c}. \end{gathered} \tag{13}$$

To solve Eq. (11), it is necessary to specify the initial partial densities of the gas on the left and right of the partition. In the gas region, the initial densities ρ_{v1} and ρ_{g1} are determined from Eqs. (5) and (6):

$$\rho_{v1} = \mu_v P_v/(RT_{g0}), \qquad \rho_{g1} = \mu_g(P - P_v)/(RT_{g0}).$$

In the mist region, the initial densities ρ_{v0} and ρ_{g0} are found from Eq. (8):

$$\rho_{v0} = \mu_v P_s(T_{v0})/(RT_{v0}), \qquad \rho_{g0} = \mu_g(P - P_s(T_{v0}))/(RT_{v0}).$$

Then, the initial conditions (1) for Eqs. (3) and (4) can be converted to the following boundary conditions for Eqs. (11) and (12):

$$\begin{aligned} &\rho_v \to \rho_{v0}, \quad \rho_g \to \rho_{g0}, \quad T \to T_{v0} \quad \text{at} \quad \xi \to -\infty, \\ &\rho_v \to \rho_{v1}, \quad \rho_g \to \rho_{g1}, \quad T \to T_{g0} \quad \text{at} \quad \xi \to +\infty. \end{aligned} \tag{14}$$

Thus, instead of the partial differential equations (3) and (4) with the initial conditions (1), we obtained the system of ordinary differential equations (11) and (12) with the boundary conditions (13) and (14).

Analysis of the Solution. The solution of Eq. (11) does not depend on Eqs. (12), and the gas distribution over the entire computation domain can be found separately in analytical form

$$\rho_g(\xi) = \rho_{g0} + \frac{\rho_{g1} - \rho_{g0}}{\sqrt{\pi}} \int\limits_{-\infty}^{\xi} \exp\left(-z^2\right) dz.$$

Using this distribution, we construct the temperature distribution in the region $\xi \leqslant \xi_s$ in implicit form

$$\rho_{g0} + \frac{\rho_{g1} - \rho_{g0}}{\sqrt{\pi}} \int\limits_{-\infty}^{\xi} \exp\left(-z^2\right) dz = \frac{\mu_g}{RT(\xi)}\Big(P - P_* \exp\Big(-\frac{T_*}{T(\xi)}\Big)\Big). \tag{15}$$

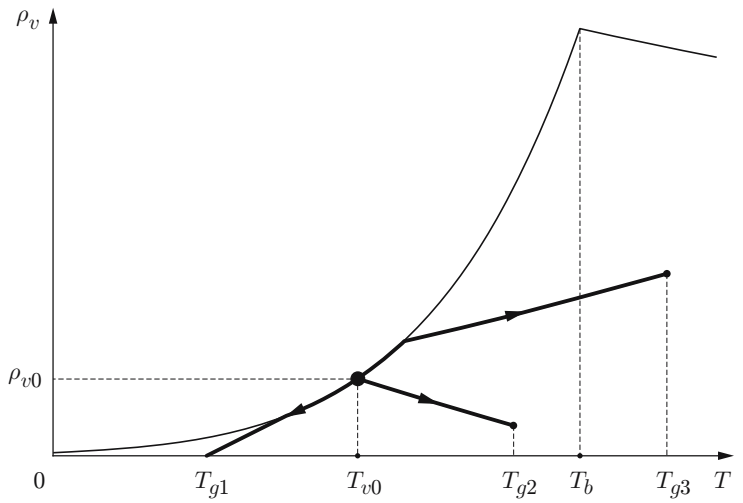

Fig. 1. Phase trajectories on the plane (T, ρ_v) for different versions of diffusion mixing of the mist and gas.

In the region $\xi > \xi_s$, the solution of Eq. (12) has the form

$$T = T_{g0} + (T_{\xi_s} - T_{g0}) \int\limits_{\xi}^{\infty} \exp(-z^2)\, dz \Big/ \int\limits_{\xi_s}^{\infty} \exp(-z^2)\, dz.$$

Using relation (15), from the heat-conduction equation (12), we obtain the following equation for ρ_l:

$$\frac{d\rho_l}{d\xi} = \frac{1}{2\xi} \frac{\rho c}{l} \frac{d^2T}{d\rho_g^2} \Big(\frac{d\rho_g}{d\xi}\Big)^2. \tag{16}$$

Equation (16) is solved numerically taking into account the condition $\rho_l = \rho_{l0}$ as $\xi \to -\infty$. The calculation is continued until the condition (13) is satisfied with the required accuracy. As a result of the solution, we obtain not only the distribution $\rho_l(\xi)$ in the region $\xi \leqslant \xi_s$ but also the coordinate of the interface ξ_s and the temperature at this interface T_s.

Analysis of Results. As an example, we consider the mixing of a water mist, consisting of a mixture of air, vapor, and water droplets, with the ambient air. The parameters determining the initial state have values typical [4] of this process: atmospheric pressure $P = 10^5$ Pa, partial density of droplets in the mist $\rho_l = 10$ g/m^3, and temperature of the mist $T_{v0} = 300$ K. The air temperature T_{g0} was varied from 273 to 400 K, and the vapor partial density in air ρ_{v1} from zero to the saturation point.

At the temperature of the mixture T for equilibrium processes, the partial vapor pressure P_v cannot exceed the saturated vapor pressure $[P_v(T) \leqslant P_s(T)]$. Figure 1 shows phase trajectories for different versions of mixing of the mist with the gas. The initial state of the mist, which is identical for all versions, is determined by the initial temperature T_{v0} and the initial density ρ_{v0}, which is equal to the saturated-vapor density at the given temperature $[\rho_{v1} = \rho_{v,s}(T_{v0})]$. This state corresponds to the initial point of the trajectory, which is in the saturation curve of $\rho_{v,s}(T)$. The mixture can contain liquid droplets in equilibrium with the vapor only at a temperature below the boiling point; therefore, in Fig. 1, the point corresponding to the initial state of the mist is to the left of the boiling point T_b.

We will consider some most typical versions for the initial state of the gas region with temperature T_{g0} and partial density ρ_{v1} that correspond to different paths of the mixing process (Fig. 1). The value of the temperature T_{g0} can be in three different regions of the temperatures T_{v0} and T_b that correspond to the mixing of the mist with a cold, warm, and hot gas. The vapor partial density ρ_{v1} at fixed temperature T_{g0} can take values in the range from $\rho_{v,s}(T)$ to zero, which corresponds to different humidities of the vapor in the gas. The terminal point of the phase trajectory corresponds to the initial state of the gas region.

1. The version $T_{g0} \leqslant T_{v0}$ corresponds to the case of mixing of the mist with a cold gas. From Fig. 1, it follows that the initial value of the vapor partial density ρ_{v1} is always lower in the gas region than in the mist

region ($\rho_{v1} < \rho_{v0}$), and, therefore, at the interface between the regions $x = x_s$, vaporization is always the case if the vapor in the gas region is unsaturated [$\rho_{v1} < \rho_{v,s}(T_{g0})$]. As the initial vapor partial density in the gas region ρ_{v1} approaches the initial value in the mist region ρ_{v0}, the vaporization rate decreases (Fig. 2a) and the temperature deficit in the mixing zone, due to heat absorption during vaporization, decreases. It is of interest to consider the case where the initial temperatures T_{v0} and T_{g0} in both regions are close or equal to each other [$T_{g0} = T_{v0}$]. In this case, vaporization leads to considerable cooling in the mixing zone and the value of $\Delta T = T_{g0} - T_s$ depends on the initial vapor partial density in the gas region ρ_{v1} (Fig. 2b).

2. The version $T_{v0} < T_{g0} < T_b$ corresponds to the case of mixing of the mist with the warm gas, whose temperature is lower than the boiling point of the liquid droplets. Variation in the temperature and vapor partial density in the mist due to the mixing with the gas, which also contains vapor, can result in condensation (Fig. 2c). Vaporization of the droplets occurs at the interface ($x = x_s$). The vaporization rate depends on two parameters: the difference between the initial temperatures $\Delta T_0 = T_{g0} - T_{v0}$, which determines the heat input to the interface depends, and the difference between the initial vapor partial pressures $\Delta\rho_v = \rho_{v1} - \rho_{v0}$, which determines the removal of the vapor produced by vaporization from the interface. The mixing zone is dominated by vaporization or condensation, depending on these parameters.

3. The version $T_{g0} \geqslant T_b$ corresponds to the case of mixing of the mist with hot gas, whose temperature is higher than the boiling point of the liquid in the droplets. As the temperature difference $\Delta T_0 = T_{g0} - T_{v0}$ increases, the vaporization rate also increases and the self-similar coordinate of the interface ξ_s is shifted to the left. As in version No. 2, the vaporization rate decreases with increasing initial vapor partial density ρ_{v1} in the gas; the latter does not exceed the partial density of the pure superheated vapor (16). However, vaporization of mist droplets is possible even if the mist is mixed with pure superheated vapor ($\rho_{v1} = \rho_{v,s}$).

Thus, the above model for the diffusion mixing of the mist with the gas in the one-dimensional formulation reveals the following features of the mixing process: if the initial temperatures of the gas and mist are close, the mixture is cooled in the mixing zone [a minimum occurs in the curve of $T(\xi)$]; if the initial temperature of the gas is higher than the initial temperature of the mist and the vapor mass concentration is higher in the gas region than in the mist region ($\rho_{v1} > \rho_{v0}$), the condensate concentration increases considerably due to the vapor supplied to the mist region from the gas region; if the initial gas temperature is higher than the boiling point of the liquid in the droplets, vaporization of the condensate occurs for all values of the initial vapor concentration in the gas (even for mixing with pure vapor).

PROBLEM OF MIXING OF A MIST CLOUD WITH AIR IN A GENERAL FORMULATION

Constitutive Equations. In this formulation, an emission cloud is considered as a mixture of air, water vapor, and condensed water consisting of droplets with a size of several micrometers, i.e., a gas–vapor–droplet mixture, which is treated as a homogeneous medium at density ρ, temperature T, and pressure P. Let $\boldsymbol{v} = \boldsymbol{v}(x, y, z, t)$ is the barycentric velocity of this medium given by the relation

$$\rho\boldsymbol{v} = \rho_a\boldsymbol{v}_a + \rho_v\boldsymbol{v}_v + \rho_l\boldsymbol{v}_l,$$

where ρ and ρ_i are the average density of the mixture and the average partial densities of the components, v_i is the velocity of the components of the mixture, and the subscripts $i = a, v$, and l refer to air, water vapor, and liquid droplets, respectively.

We introduce the mass-average concentrations of the components of the gas–droplet mixture $k_i = \rho_i/\rho$ that satisfy the condition

$$k_a + k_v + k_l = 1. \tag{17}$$

The average density of the mixture can be expressed in terms of the true densities of the liquid ρ_l^0 and the vapor–gas mixture ρ_g^0 [6]:

$$\frac{1}{\rho} = \frac{k_l}{\rho_l^0} + \frac{1 - k_l}{\rho_g^0}. \tag{18}$$

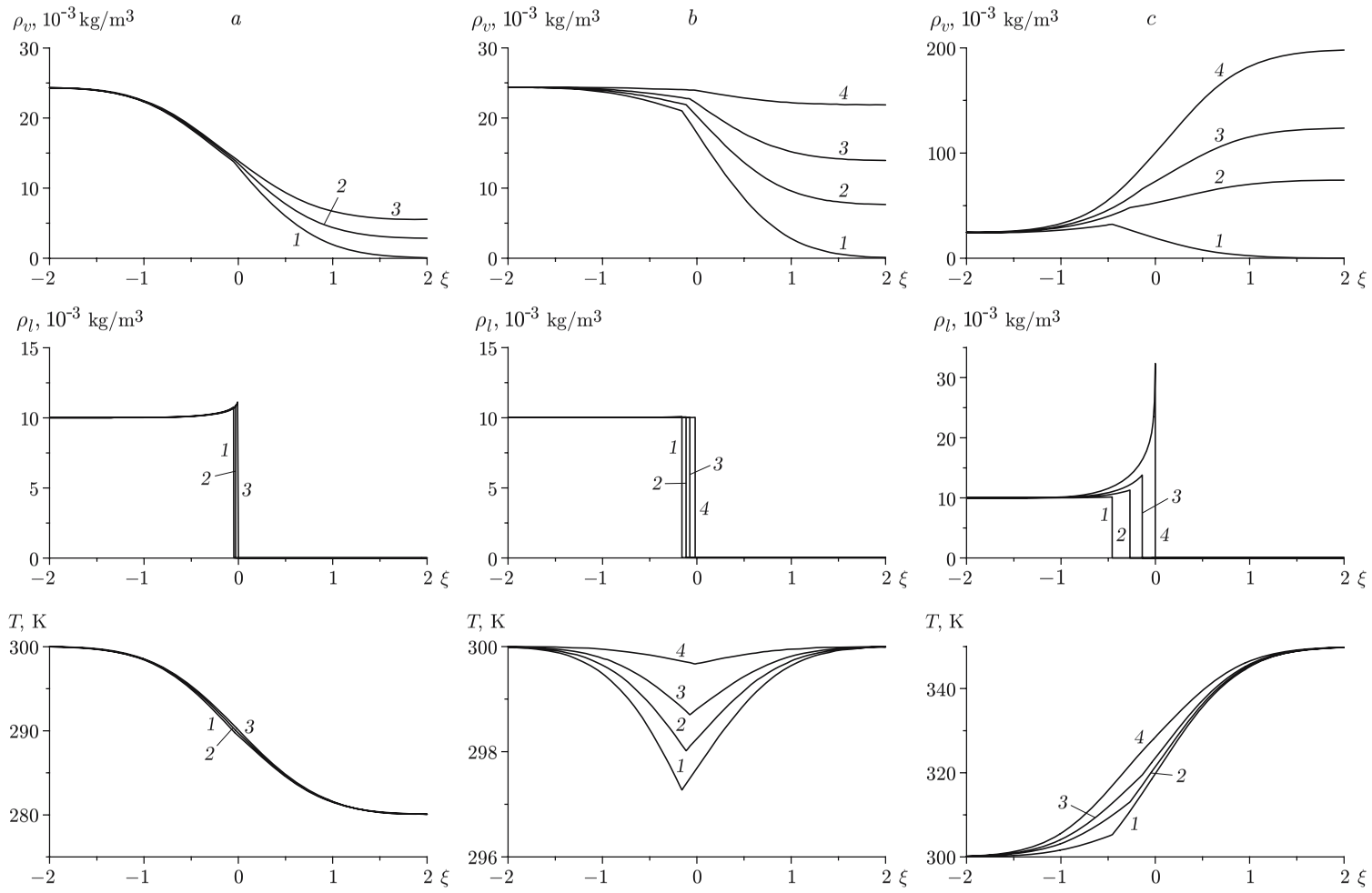

Fig. 2. Partial densities of vapor (ρ_v) and droplets (ρ_l) and temperature T in the mixture for mixing of mist and gas: (a) cold gas at $\rho_{v1} = 0$ (1), 2.9 $\cdot 10^{-3}$ (2), and 5.5 $\cdot 10^{-3}$ kg/m^3 (3); (b) warm gas at $\rho_{v1} = 0$ (1), 7.6 $\cdot 10^{-3}$ (2), 13.9 $\cdot 10^{-3}$, and 21.8 $\cdot$ 10^{-3} kg/m^3 (4); (c) hot gas at $\rho_{v1} = 0$ (1), 74.2 $\cdot 10^{-3}$ (2), 123.7 $\cdot$ 10^{-3} (3), and 197.8 $\cdot$ 10^{-3} kg/m^3 (4).

Along with the concentrations k_i, we introduce the true concentrations of air and vapor in the gas part of the mixture k_i^0 $(i = a, v)$; in this case, $k_a^0 + k_v^0 = 1$. Obviously, the average and true concentrations are related as

$$k_a = (1 - k_l)k_a^0, \qquad k_v = (1 - k_l)k_v^0. \tag{19}$$

If droplets are absent ($k_l = 0$), i.e., if the dew point is not reached, the average and true concentrations coincide ($k_i = k_i^0$). Assuming that the gas mixture obeys the Dalton law, we write the equation of state as

$$P = \rho_g^0 R_g T, \qquad R_g = R(k_v^0/\mu_v + k_a^0/\mu_a).$$

From relations (17)–(19), we obtain the equation of state for the mixture as a whole:

$$\frac{1}{\rho} = \frac{k_l}{\rho_l^0} + \frac{RT}{P}\Big(\frac{k_v}{\mu_v} + \frac{k_a}{\mu_a}\Big). \tag{20}$$

We assume that the vapor in the gas mixture and the liquid in the droplets are in thermodynamic equilibrium, so that the partial pressure P_v is equal to the saturation pressure at the current temperature T $[P_v = P_s(T)]$. In this case, the water vapor saturation curve is given by relation (7). The vapor partial pressure can be written as

$$P_v = \rho_g^0 R_v T,$$

where $R_v = Rk_v^0/\mu_v$. At a given temperature of the mixture, the value of P_v cannot exceed the saturated-vapor pressure. Therefore, the mass-average concentration of water vapor in the mixture k_{vs} has an upper limit, which is determined from relation (20) under the assumption that $P_v = P_s(T)$. We also introduce the notion of the saturation temperature $T_s = T_*/\ln(P/P_v)$ which corresponds to the given value of the vapor partial pressure p_v. In meteorology, the relative air humidity $\varphi = P_v/P_s(T)$ is used. In the present work, this quantity is used to analyze calculation results.

The above assumptions and notation underlie the following theoretical model for the atmospheric diffusion of emissions containing water vapor. For the mixture as a whole, the continuity equation is written as

$$\frac{\partial \rho}{\partial t} + \nabla^k(\rho v^k) = 0. \tag{21}$$

The mixing of the two-phase vapor–gas–droplet mixture considered will be described in a diffusion approximation [6]. For this, we introduce the diffusion velocities of the components $\boldsymbol{w}_i = \boldsymbol{v}_i - \boldsymbol{v}$ $(i = a, v, l)$ subject to the condition

$$\rho_a \boldsymbol{w}_a + \rho_v \boldsymbol{w}_v + \rho_l \boldsymbol{w}_l = 0. \tag{22}$$

Then, for the relative motion of the air component of the mixture, we write generalized Fick's law as

$$\rho_a w_a^k = -\rho D^{kn} \nabla^n k_a \qquad (\rho_a = \rho k_a),$$

where D^{kn} is the square matrix of the diffusion coefficients, which is considered to be diagonal (diffusion in the horizontal and vertical directions arises if the concentration in these directions is nonuniform).

In Eq. (22), we set $\boldsymbol{w}_l = 0$, i.e., the droplets move at the mass-average velocity ($\boldsymbol{v}_l = \boldsymbol{v}$). Then, the vapor diffuses toward the air at relative velocity $\boldsymbol{w}_v$, which is determined from the expression

$$\rho_v \boldsymbol{w}_v = -\rho_a \boldsymbol{w}_a.$$

Within the framework of these assumptions, from the mass conservation law for the air and droplets, we obtain the equations

$$\rho \frac{dk_a}{dt} = \nabla^k\Big(\rho D^{kn} \nabla^n k_a\Big), \qquad \rho \frac{dk_l}{dt} = J, \tag{23}$$

where J is the vapor condensation rate in unit volume, which is determined from the heat-balance equation [9] (see below).

The motion of the mixture of the vapor, air, and droplets is described by the momentum equation with gravity and turbulent viscosity taken into account:

$$\rho \frac{dv^k}{dt} = -\nabla^k P + \rho g^k + \nabla^n(\tau^{kn}). \tag{24}$$

Here τ^{kn} are elements of the reduced shear stress tensor which describe momentum transfer.

We write the heat-balance equation with the turbulent hear transfer and phase transition taken into account:

$$\rho c \frac{dT}{dt} = \nabla^k(\lambda^{kn}\nabla^n T) + Jl. \tag{25}$$

Here λ^{kn} are elements of the matrix of thermal conductivities and l is the latent heat of the phase transition. The specific thermal conductivity of the mixture is given by

$$c = k_a c_a + k_v c_v + k_l c_l,$$

where c_a, c_v, and c_l are the specific heats of the air, vapor, and droplets, respectively, at constant pressure.

Thus, the mathematical model taking into account the convective and turbulent transfer of mass, momentum, and energy and condensation and vaporization of water vapor consists of Eqs. (20), (21), and (23)–(25).

The system consisting of Eqs. (20), (21), (23)–(25) is closed using the semiempirical theory of turbulent diffusion based on the k-model [10, 11], in which the turbulent transfer coefficients are linked to the altitude in the surface layer of the atmosphere by the empirical formulas

$$D_{xx} = D_{yy} = k_0 v_1 \ln(z/z_0 + 1), \qquad D_{zz} = k_1 z/z_1.$$

The empirical constants k_0, v_1, z_1, z_0, and k_1 are determined by the state of the surface atmospheric layer.

The relationship between the turbulent transfer processes is established via the turbulent Prandtl number Pr and Schmidt number Sc, which are usually set equal to unity [5]. Then,

$$\lambda^{kn}/(\rho c) = \mu^{kn}/\rho = D^{kn}.$$

We will also assume that the coefficients D^{kn} inside the vapor cloud coincide with the background values for the ambient medium since this is preceded by the stage of cloud formation as a result of impurity emission and mixing with the ambient air.

Initial Conditions. We consider a vapor–condensate cloud in the shape of a cube (for convenience of calculations on a rectangular grid) produced by emission. At the initial time $t = 0$, the ambient temperature T_a is uniform over the entire computation domain and the pressure is given by the distribution

$$P_a(x, y, z, 0) = P_{a0} \exp(-\mu_a g z/(RT_a)),$$

where P_{a0} is the normal atmospheric pressure. At the initial time, the velocity of the cloud is zero over the entire computation domain: $\boldsymbol{v} = \boldsymbol{v}(x, y, z, 0) = 0$.

The ambient air contains a water vapor, whose concentration is determined by the relative humidity φ and temperature T_a. At the initial time, the pressure distribution in the water vapor cloud corresponds to the pressure distribution in the ambient air. In the cloud, the vapor temperature T_g is uniform and differs from ambient air temperature. The vapor in the cloud is saturated because of the presence of water droplets.

The system of equations is solved numerically using the particle-in-cell method [12]. This method is used to solve a wide class of problems of fluid dynamics and belongs to methods of splitting the basic unsteady system of equations in physical processes. A description of this numerical scheme for atmospheric emissions is given in [13]. In the present study, this scheme is extended to the case of phase transitions.

In spite the large number of equations and parameters considered, a representation of the mixture of an air vapor and water droplets as a unified cloud allows the problem of motion of the cloud to be solved numerically with adequate accuracy on a personal computer using the particle-in-cell technique.

The stability and adequacy of the numerical solution method was tested in [12]. In the present work, we tested the numerical scheme by solving problems which have analytical solutions (for example, the diffusion problem) and found the values of the steps in time and coordinate that satisfy the Courant condition.

Calculation Results. For a quantitative analysis, the surface separating the region with droplets and the region without droplets is taken to be the conditional boundary of the cloud. The water vapor region containing droplets (or condensate), i.e., the region consisting of air, vapor, and droplets, will be called a mist cloud.

Cold atmospheric air penetrates trough the boundary into the cloud, changing the humidity, on the one hand, and the heat balance in the cloud, on the other hand.

The motion of the emission cloud is influenced by external factors: the air temperature and humidity and wind speed and direction. In all calculations, the parameters of the cloud in the initial state and the temperature and concentration of the condensate in the cloud are assumed to be identical. Therefore, in the numerical experiments, as

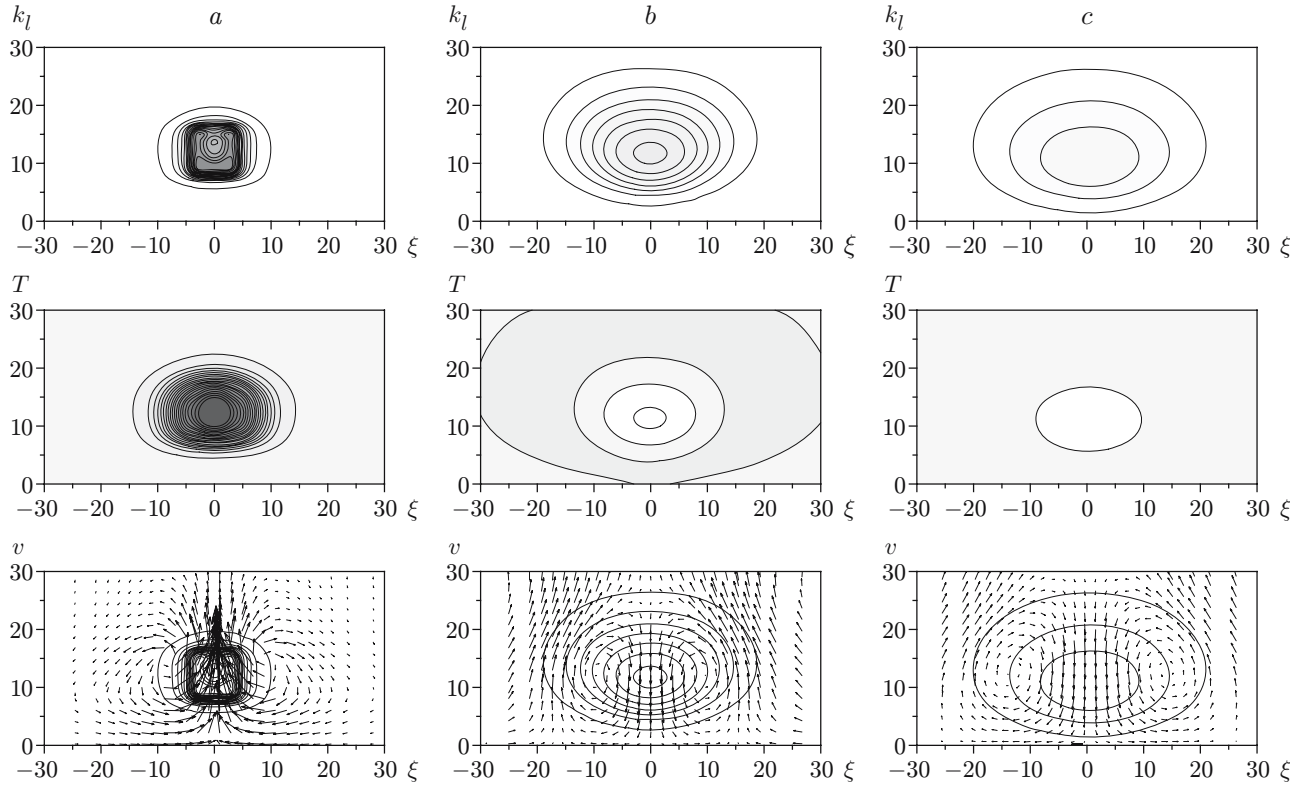

Fig. 3. Fields of mass-average droplet concentration k_l, temperature T, and velocity v at $t = 1$ (a), 20 (b), and 35 sec (c).

varied parameters we use the temperature T_a and relative humidity φ of the ambient air and the initial mass-average concentration of droplets k_{l0} in the cloud.

The main parameters of the cloud that determine its further evolution (the condensate mass in the cloud m_l, the minimum temperature in the cloud $T_{\min}$, and the maximum density of the mixture in the cloud $\rho_{\max}$ are calculated during numerical experiments.

Let us consider the motion of the mist cloud which, at the initial time, is at altitude h above the underlying surface. The initial temperature of the cloud is close to but lower (because of the presence of liquid droplets) than the boiling point of water ($T_g = 370$ K). For the calculations, we use two values of the initial air temperature: $T_a = 300$ K (warm weather) and $T_a = 280$ K (cold weather) and two values of the relative air humidity characteristic of the middle latitudes in dry ($\varphi = 60\%$) and wet ($\varphi = 90\%$) weather.

The visible shape of the cloud is determined by the water droplet distribution in the cloud, i.e., by the mass-average droplet concentration k_l (Fig. 3). From the calculation results, one can examine the evolution of the shape of the cloud in the three-dimensional form. On the boundary of the cloud, the hot mist and cold air are mixed with subsequent water condensation. When the cloud temperature decreases to values close to the ambient air temperature, water begins to vaporize and the cloud gradually diffuses.

The evolution of the temperature field in the computation domain depend greatly on the condensation and vaporization processes (Fig. 3). In the initial stage, the temperature field changes only slightly due to release of the latent heat of vaporization. Subsequently, the cold and drier air penetrating into the cloud increases the vaporization rate. Because of the heat losses due to vaporization, the cloud temperature drops below the ambient air temperature and a temperature minimum forms.

The mixing of the hot vapor with the ambient air leads to a complex structure of the velocity field of the medium (Fig. 3). In the initial state, despite the presence of the condensate, the hot mist is almost twice lighter than the ambient air, resulting in the formation of an upward flow. In this case, the flow velocity reaches several meters per second in the first second of motion. Cold air enters the lower part of the cloud, and the upper, warmer

part of the cloud mounts rises up. As the cloud is cooled, the vertical velocity component becomes negative — the mixture becomes heavier than air and settles on the underlying surface (Fig. 3).

Thus, the proposed theoretical model provides a three-dimensional representation of the motion of the mist cloud in the surface atmospheric layer and reveals the main features of this motion.

In the initial stage of mixing of the cloud with cold air ($t < 2$ sec), the vapor is cooled and rapidly condensed, resulting in an increase in the liquid phase concentration. In the next stage (2 sec $< t <$ 10 sec), mixing with the ambient dry air leads to rapid vaporization of the droplets. The cooling process induced by the entry of cold air to the cloud is accompanied by heat absorption during vaporization. Although the initial temperature is close to the boiling point, the temperature in the cloud drops below the ambient temperature T_a. Calculations have shown that the cloud is cooled to the temperature $T < T_a$ only in the presence of condensate in the initial composition of the cloud. The value of $\Delta T = T_{\min} - T_a$ (Fig. 4) depends on the initial droplet concentration in the cloud k_{l0} and the ambient air humidity φ. The final stage involves ($t > 10$ sec) dilution of the cloud with the ambient air and gradual heating and complete vaporization of the droplets. In this stage, the slope of the curve $m_l(t)$ is determined by the droplet vaporization rate.

The indicated changes in the condensate mass and cloud temperature during mixing with the ambient air result in a change in the density of the mixture (Fig. 4), which determines the buoyancy of the cloud. The maximum density in the cloud is 10% higher than the density of the ambient air. The flow velocities in the cloud are directed downward (see Fig. 3).

An increase in the density is facilitated by a decrease in the cloud temperature below the air temperature. Quantitative estimates show that approximately half of the density increment is due to an increase in the mass of the condensate, and the other half is due to the temperature drop. The initial condensate concentration in the cloud determines an increase in the droplet mass and the value of ΔT.

Thus, the presence of the condensate in the initial cloud results in a change in the nature of motion of the emission: with time, the cloud acquires negative buoyancy. Calculations show that the cloud settling velocity is relatively low (≈20 cm/sec) and a long time is required for the cloud to move a considerable distance.

For an ambient air humidity of $\varphi = 90\%$, the maximum density in the cloud is almost the same as for $\varphi = 60\%$, although the absolute mass of the condensate increases. Obviously, the increase in the condensate mass is due to an increase in the cloud volume. The time of vaporization of the cloud, during which it settles slowly and is accumulated in the form of a mist, increases to 100 sec. This development scenario is the most hazardous to the environment because the condensate droplets combine with the harmful emission components (for example, SO_2) and solid smoke particles to form a smog.

An analysis of the curves of $T_{\min}(t)$ and $\rho_{\max}(t)$ at $T_a = 280$ K shows that, on the one hand, the absolute value of vapor density (see Fig. 4) increases compared to the corresponding value at $T_a = 300$ K, and, on the other hand, the relative increase in the density $\Delta\rho/\rho_a$, which determines the negative buoyancy force, remains almost unchanged. Consequently, although a change in the ambient air temperature leads to a considerable increase in the condensate mass in the cloud, it has little effect on the behavior of the cloud. The buoyancy and time of vaporization of the cloud remain almost unchanged.

The numerical modeling of the diffusion of the vapor–gas–droplet mixture in the surface atmospheric layer show that, despite the minor contribution of the condensate to the average density of the mixture in the initial state, its presence in the emission cloud is responsible for substantial heat absorption during vaporization, resulting in the cloud cooling to a temperature below the ambient air temperature. This, in turn, leads to an increase in the density and the formation of a mixture whose mass is greater than the mass of the air surrounding the cloud. Subsequently, this cloud settles on the underlying surface and can be accumulated as a mist.

The main external factor that has a significant effect on the motion of the cloud is found to be the relative humidity of the ambient air. Although a decrease in the ambient air temperature leads to a considerable increase in the condensate mass in the cloud, this does not affect the nature of motion of the emissions since the buoyancy and time of vaporization of the cloud change only slightly.

Conclusions. The mixing of the vapor–gas–droplet mixture with gas was studied using analytical and numerical models. The analytical solution of the problem in the one-dimensional formulation predicts a considerable decrease in the temperature of the mixture in the mixing zone due to heat absorption during vaporization. The vaporization rate is determined primarily by the humidity of the gas and only slightly by the gas temperature. The

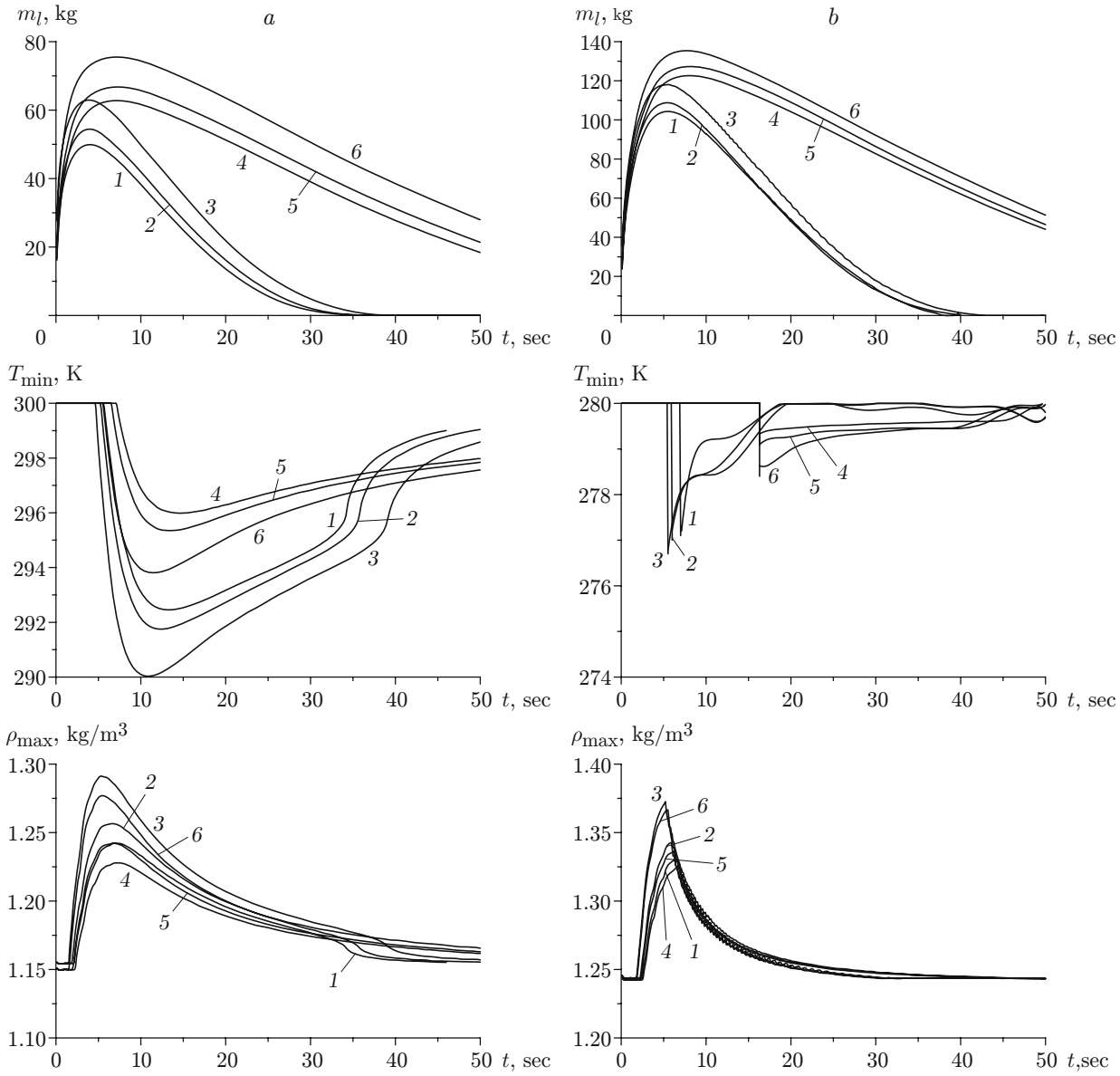

Fig. 4. Condensate mass m_l, minimum cloud temperature $T_{\min}$, and maximum partial density of droplets in the cloud $\rho_{\max}$ in the case of mixing of the mist with air in warm (a) and cold (b) weather: curves 1–3 refer to $\varphi = 60\%$ and $k_{l0} = 0.01$ (1), 0.02 (2), and 0.04 (3); curves 4–6 refer to $\varphi = 90\%$ for $k_{l0} = 0.01$ (4), 0.02 (5), and 0.04 (6).

numerical calculations in the three-dimensional formulation confirmed that the presence of the condensate in the vapor cloud in the initial state results in the cooling of the mixing zone to a temperature below the ambient air temperatures, which causes a change in the nature of motion of the cloud (the buoyancy of the cloud changes sign from positive to negative). This effect is enhanced with increasing humidity of the ambient air.

REFERENCES

1. S. Calvert and H. M. Englund, *Handbook of Air Pollution Control Technology*, John Wiley and Sons, New York (1988).
2. G. I. Marchuk, *Mathematical Modeling in Environmental Problems* [in Russian], Nauka, Moscow (1981).

3. V. V. Penenko and A. E. Aloyan, *Models and Methods for Environmental Problems* [in Russian], Nauka, Novosibirsk (1985).
4. L. T. Matveev, *A Course in General Meteorology. Atmospheric Physics* [in Russian], Gidrometeoizdat, Leningrad (1976).
5. L. G. Loitsyanskii, *Mechanics of Liquids and Gases*, Pergamon Press, Oxford–New York (1966).
6. R. I. Nigmatulin, *Dynamics of Multiphase Media*, Part 1, Hemisphere, New York (1991).
7. P. P. Volosevich and E. I. Levanov, *Self-Similar Solutions of Problems of Gas Dynamics and Heat Transfer* [in Russian], Fizmatlit, Moscow (1997).
8. A. N. Tikhonov and A. A. Samarskii, *Equations of Mathematical Physics* [in Russian], Izd. Mosk. Univ.–Nauka, Moscow (2004).
9. I. M. Bayanov, I. R. Khamidullin, and V. Sh. Shagapov "Behavior of an emission cloud of high humidity in the surface atmospheric layer," *Teplofiz. Vysok. Temp.*, **45**, No. 2, 267–276 (2007).
10. M. E. Berlyand, *Modern Problems of Atmospheric Diffusion and Pollution* [in Russian], Gidrometeoizdat, Leningrad (1975).
11. A. S. Monin, "Semi-empirical theory of turbulent diffusion," in: *Tr. Geofiz. Inst. Akad Nauk SSSR*, No. 33, 3–47 (1956).
12. O. M. Belotserkovskii and Yu. M. Davydov, *Particle-in-Cell Method in Gas Dynamics* [in Russian], Nauka, Moscow (1982).
13. I. M. Bayanov, M. Z. Gilmullin, and V. Sh. Shagapov, "Calculation of heavy gas spreading overt the earth surface by a three-dimensional model," *J. Appl. Mech. Tech. Phys.*, **44**, No. 6, 858–865 (2003).